Supplementary Material Available: Tables of crystal data, fractional coordinates, isotropic and anisotropic thermal parameters, bond distances, bond angles, and ring centroid calculations pertaining to the X-ray crystallographic study of **9** (9 pages); a listing of observed and calculated structure factors (13 pages). Ordering information is given on any current masthead page.

Electrochemical and Spectroelectrochemical Studies of (TPP)[Ir(CO)₃]₂ in Nonaqueous Media

K. M. Kadish,* Y. J. Deng, C.-L. Yao, and J. E. Anderson

Department of Chemistry, University of Houston, Houston, Texas 77204-5641

A modified method for the synthesis of (TPP)[Ir(CO)₃]₂ from [Ir(CO)₃Cl]₂ and (TPP)H₂ where TPP is the dianion of tetraphenylporphyrin was developed and gives a much higher percent yield. Electrochemical and spectroelectrochemical studies of (TPP)[Ir(CO)₃]₂ indicate that this binuclear Ir(I) complex undergoes two reversible reductions at the porphyrin π-ring system. Three irreversible oxidations are observed in benzonitrile containing 0.2 M tetrabutylammonium perchlorate, while in CH₂Cl₂, only two irreversible oxidations are recorded. The first oxidation occurs at one of the two Ir(I) centers of (TPP)[Ir(CO)₃]₂ and is followed by a rapid chemical reaction that leads to the generation of [(TPP)Ir]⁺ClO₄⁻ or a solvated form of this species in solution. An overall mechanism for the electrochemical conversion of binuclear (TPP)[Ir(CO)₃]₂ to monomeric [(TPP)Ir]⁺ClO₄⁻ and the additional reactions of this species are reported. Comparisons are also made between electrochemical properties of binuclear (TPP)[Ir(CO)₃]₂ and the binuclear Rh(I) analogue (TPP)[Rh(CO)₂]₂.

Introduction

Rhodium porphyrins have demonstrated their ability to undergo a variety of interesting chemical and electrochemical reactions.[1-8] Similar types of reactions may also occur with iridium porphyrins,[9,10] but detailed comparisons between rhodium and iridium porphrins have, in general, not been possible due to the small amount of data available for the iridium complexes. In this regard, studies of iridium porphyrins have generally been hampered by the fact that the synthesis gives relatively low yields and typically results in formation of several different side products.[11-15]

This is in contrast to rhodium porphyrins that are generally synthesized in good yields and in high purity.[16]

Recently, the electrochemistry of a binuclear Rh(I) porphyrin was reported.[17] The one-electron oxidation of (P)[Rh(CO)₂]₂ is followed by a metal insertion reaction with the ultimate formation of [(P)Rh]⁺ in solution. It was not clear if this electrochemically initiated insertion is specific to the oxidized binuclear Rh(I) complex or if other binuclear porphyrins containing metals in the +1 oxidation state might possess the same reactivity. This is examined in this paper which reports the first electrochemistry of a binuclear iridium porphyrin as well as an improved method for the synthesis of (TPP)[Ir(CO)₃]₂. Electrochemical and spectroelectrochemical results are coupled with ESR studies to give a self-consistent mechanism for oxidation and reduction of this binuclear compound in nonaqueous media.

Experimental Section

Chemicals. Reagent grade benzonitrile (PhCN) was vacuum distilled from P₂O₅ while spectroscopic grade dichloromethane

(1) Ogoshi, H.; Setsune, J.; Yoshida, Z. *J. Am. Chem. Soc.* **1979**, *99*, 3869.

(2) Wayland, B. B.; Del Rossi, K.; *J. Organomet. Chem.* **1984**, *276*, C27.

(3) Paonessa, R. S.; Thomas, N. C.; Halpern, J. *J. Am. Chem. Soc.* **1985**, *107*, 4333.

(4) van Voorhees, S. L.; Wayland, B. B. *Organometallics* **1985**, *4*, 1887.

(5) Kadish, K. M.; Yao, C.-L.; Anderson, J. E.; Cocolios, P. *Inorg. Chem.* **1985**, *24*, 4515.

(6) Anderson, J. E.; Yao, C.-L.; Kadish, K. M. *J. Am. Chem. Soc.* **1987**, *109*, 1106.

(7) Anderson, J. E.; Yao, C.-L.; Kadish, K. M. *Organometallics* **1987**, *6*, 706.

(8) Hughes, R. P. *Comprehensive Organometallic Chemistry*; Wilkinson, G., Ed.; Pergamon: New York, 1982; Vol. 5, p 388.

(9) van Baar, J. F.; van Veen, J. A. R.; Dewit, N. *Electrochim. Acta* **1982**, *27*, 57.

(10) Farbis, M. D.; Woods, B. A.; Wayland, B. B. *J. Am. Chem. Soc.* **1986**, *108*, 3659.

(11) Fleischer, E. B.; Sadasivan, N. *Chem. Commun.* **1967**, *22*, 159.

(12) Sadasivan, N.; Fleischer, E. B. *J. Inorg. Nucl. Chem.* **1968**, *30*, 591.

(13) Sugimoto, H.; Ueda, N.; Mori, M. *J. Chem. Soc. Dalton Trans.* **1982**, 1611.

(14) Cornillon, J.-L.; Anderson, J. E.; Swistak, C.; Kadish, K. M. *J. Am. Chem. Soc.* **1986**, *108*, 7633.

(15) Ogoshi, H.; Setsune, J.; Yoshida, Z. *J. Organomet. Chem.* **1978**, *159*, 317.

(16) Fleischer, E. B.; Dixon, F. L.; Florida, R. *Inorg. Nucl. Chem. Lett.* **1973**, *9*, 1303.

(17) Yao, C.-L.; Anderson, J. E.; Kadish, K. M. *Inorg. Chem.* **1987**, *26*, 2725.

(18) Yoshida, Z.; Ogoshi, H.; Omura, R.; Watanabe, E.; Kurosaki, T. *Tetrahedron Lett.* **1972**, 1077.

Table I. Maximum Absorbance Wavelengths (λ_{max}) and Corresponding Molar Absorptivities (ϵ) for the Oxidized and Reduced Products of (TPP)[Ir(CO)$_3$]$_2$ in CH$_2$Cl$_2$ and PhCN Containing 0.2 M TBAP

compd	solv	λ_{max}, nm ($10^{-3}\epsilon$)				
(TPP)[Ir(CO)$_3$]$_2$	CH$_2$Cl$_2$	358 (46.6)	454 (119)	564 (14.5)	610 (17.1)	662 (11.2)
	PhCN	360 (44.4)	457 (120)	564 (11.9)	614 (11.5)	662 (10.9)
(TPP)[Ir(CO)$_3$]$_2^-$	CH$_2$Cl$_2$	415 (72.4)	444 (62.8)	476 (50.1)		
	PhCN	423 (68.6)	447 (83.7)	566 (15.3)		
(TPP)[Ir(CO)$_3$]$_2^{2-}$	CH$_2$Cl$_2$	413 (72.7)	478 (95.4)			
	PhCN	442 (29.6)	670 (24.0)			
[(TPP)Ir]$^+$ [a]	CH$_2$Cl$_2$	413 (343)	524 (34.2)			
	PhCN	416 (280)	527 (32.4)			
[(TPP)Ir]$^{2+}$ [b]	CH$_2$Cl$_2$	411 (166)	570 (17.7)	628 (18.3)		
	PhCN	416 (287)	582 (15.0)	635 (16.9)		

[a] Generated by controlled potential oxidation of (TPP)[Ir(CO)$_3$]$_2$ at +1.20 V. [b] Generated by controlled potential oxidation of (TPP)[Ir-(CO)$_3$]$_2$ at +1.50 V.

(CH$_2$Cl$_2$) was distilled from CaH$_2$. Tetra-n-butylammonium perchlorate (TBAP) (Fluka Co.) was twice recrystallized from ethyl alcohol and stored in a vacuum oven at 40 °C. [Ir(CO)$_3$Cl]$_2$ was purchased from Strem Chemicals, Inc., and used without further purification.

Instrumentation. Cyclic voltammetric measurements were performed with a conventional three-electrode system using an IBM 225 voltammetric analyzer. The working electrode was a platinum button of 0.88 mm^2 area. A saturated calomel electrode (SCE) was used as the reference electrode for all electrochemical and UV–visible spectroelectrochemical experiments. In the case of FTIR/electrochemical experiments, an Ag/AgCl electrode was used as the reference. Details for construction of the thin-layer spectroelectrochemical cell have been reported in the literature.[19] A Tracor Northern 1710 holographic optical spectrometer was used to obtain UV–visible spectra. IR spectra were taken on an IBM 32 FT-IR spectrophotometer. ESR spectra were recorded on an IBM Model ER-100D electron spin resonance system.

Synthesis of (TPP)[Ir(CO)$_3$]$_2$. (TPP)[Ir(CO)$_3$]$_2$ was synthesized by a method similar to the one reported for (P)[Rh-(CO)$_2$]$_2$[18] and was carried out as follows: A mixture of 500 mg of (TPP)H$_2$ and 600 mg of [Ir(CO)$_3$Cl]$_2$ in 500 mL of benzene containing 50 mL of methanol was stirred at 35 °C for 10 h. Methanol was added to the benzene to increase the solubility of [Ir(CO)$_3$Cl]$_2$. The reaction was protected from light for the entire period and was monitored by thin-layer chromatography. Upon completion of the reaction, unreacted [Ir(CO)$_3$Cl]$_2$ was recovered by filtration. The remaining solution was evaporated and the reaction mixture separated on a silica gel column with CH$_2$Cl$_2$ as eluant. The first eluate was unreacted (TPP)H$_2$, and this was followed by small amounts of (TPP)Ir(CO)Cl (20 mg after recrystalization). A green band that corresponded to (TPP)[Ir(C-O)$_3$]$_2$ was eluted with a CH$_3$OH/CH$_2$Cl$_2$ mixture (1:100). This product was further purified on a silica gel column using C$_6$H$_6$, followed by recrystallization from a mixture of CH$_2$Cl$_2$ and hexane. The unreacted (TPP)H$_2$ and [Ir(CO)$_3$Cl]$_2$ could then be recycled to increase the yield. A single reaction gave 25% yield of (TPP)[Ir(CO)$_3$]$_2$ after purification based on the possible mass of product calculated from the mass of initial iridium starting material. The UV–visible spectrum of this species in both CH$_2$Cl$_2$ and PhCN is reported in Table I, and the infrared spectrum had CO stretching bands at 2054 and 1979 cm^{-1}. These spectral characteristics match those previously reported for this complex.[15,18]

Results and Discussion

Synthesis of Binuclear Iridium Porphyrins. Previous reports for the synthesis of (P)[Ir(CO)$_3$]$_2$ involve isolation of this product from a general metal insertion reaction. Under these conditions, the synthesis gives a 3.5% yield.[15,18] In the present synthesis, a 25% yield was obtained after purification. The only side product in the reaction is (TPP)Ir(CO)Cl which is recovered in 3% yield. The increase in yield from 3.5 to 25% for (P)[Ir(CO)$_3$]$_2$ is due to the lower temperature utilized (35 °C vs 140 °C in
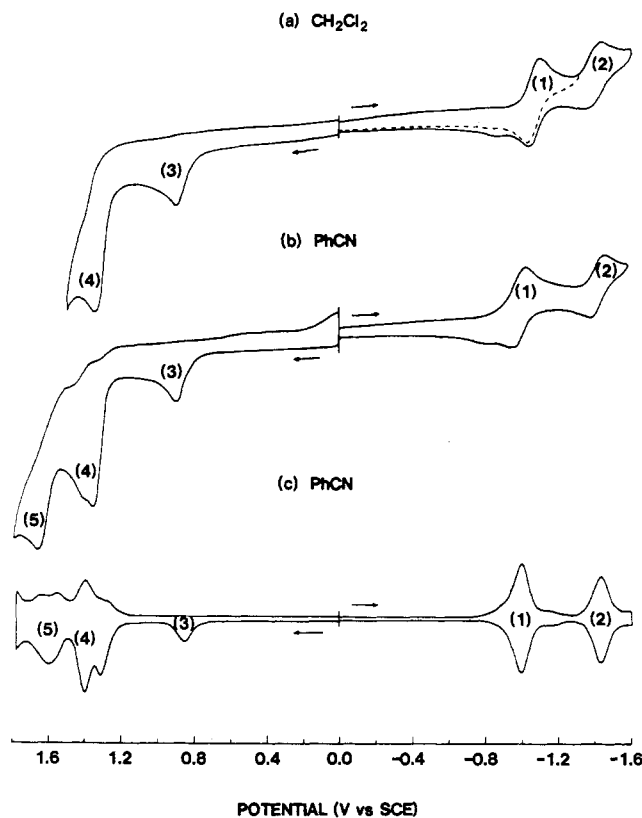
(19) Lin, X. Q.; Kadish, K. M. *Anal. Chem.* **1985**, *57*, 1498.

Figure 1. Cyclic voltammograms of (a) 6.9 × 10^{-4} M (TPP)-[Ir(CO)$_3$]$_2$ in CH$_2$Cl$_2$, 0.2 M TBAP (scan rate = 0.1 V/s), (b) 9.5 × 10^{-4} M (TPP)[Ir(CO)$_3$]$_2$ in PhCN, 0.2 M TBAP (scan rate = 0.1 V/s), and (c) differential pulse voltammogram of 9.5 × 10^{-4} M (TPP)[Ir(CO)$_3$]$_2$ in PhCN, 0.2 M TBAP (modulation amplitude = 0.005 V; scan rate = 0.005 V/s).

the literature[15,18]) as well as to the fact that the reaction mixture was protected from light. (TPP)[Ir(CO)$_3$]$_2$ was found to be extremely sensitive to UV light (λ < 350 nm) and slightly sensitive to visible light.[20]

Electroreduction of (TPP)[Ir(CO)$_3$]$_2$. A cyclic voltammogram of (TPP)[Ir(CO)$_3$]$_2$ shows two oxidations and two reductions in CH$_2$Cl$_2$, 0.2 M TBAP. The same reactions are observed in PhCN, but a third oxidation process also occurs in this solvent due to the more positive solvent window. In addition, there is a small irreversible

(20) Photodecomposition of (TPP)[Ir(CO)$_3$]$_2$ results in the formation of (TPP)Ir(CO)Cl. This product was identified by UV–visible and infrared spectra of products obtained after irradiation with light at various wavelengths.[21] Quantum yields for formation of (TPP)Ir(CO)Cl were virtually identical at 455, 610, and 660 nm and were in the range of (1.5–2.5) × 10^{-3}.

(21) Swistak, C.; Cornillon, J.-L.; Anderson, J. E.; Kadish, K. M. *Organometallics* **1987**, *6*, 2146.
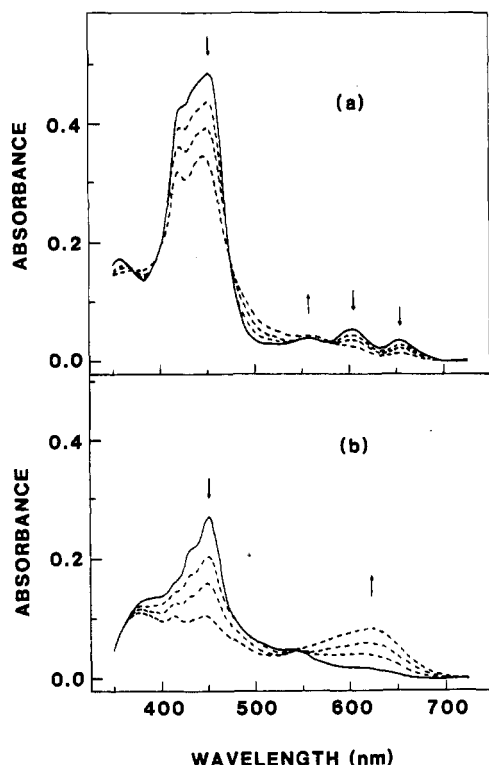
Figure 2. UV–visible spectral changes during controlled potential reduction of 1.5×10^{-4} M (TPP)[Ir(CO)₃]₂ in PhCN, 0.2 M TBAP, at (a) –1.20 V and (b) –1.65 V.

oxidation at E_{pa} = –0.84 V when the potential is scanned negative of the second reduction peak in either CH₂Cl₂ or PhCN.

The first two reductions of (TPP)[Ir(CO)₃]₂ (labeled processes 1 and 2 in Figure 1) are located at $E_{1/2}$ = –0.99 and –1.42 V in PhCN and at $E_{1/2}$ = –1.07 and –1.40 V in CH₂Cl₂. Both reactions are reversible diffusion-controlled processes as demonstrated by an $|E_{pa} - E_{pc}|$ = 60 ± 10 mV and a constant value of $i_p/v^{1/2}$.

The two reductions of (TPP)[Ir(CO)₃]₂ are also reversible by differential pulse voltammetry. This is shown in Figure 1c. Bulk electrolysis and thin-layer coulometery give 1.2 ± 0.1 electrons added in the first reduction and 1.6 ± 0.1 electrons added in the second reduction. The increased coulometric value of n in the second process may be due to reduction of impurities in the solvent or to a decomposition of the porphyrin dianion followed by a further reduction of the reaction products.

Figure 2 shows changes that occur in the UV–visible spectra of (TPP)[Ir(CO)₃]₂ in PhCN during stepwise controlled potential electrolysis at –1.20 and –1.65 V. The initial complex has a broad absorption at 457 nm and other bands at 360, 564, 614, and 662 nm. The singly reduced product (Figure 2a) has bands at 423, 447, and 566 nm. The addition of a second electron at –1.65 V results in a decrease of the bands at 423, 447, and 566 nm and the appearance of a broad absorption at 670 nm. This is shown in Figure 2b, and the spectral data for (TPP)[Ir(CO)₃]₂⁻ and (TPP)[Ir(CO)₃]₂²⁻ are summarized in Table I.

The spectral data in parts a and b of Figure 2 are consistent with consecutive one-electron transfers to form a porphyrin π-anion radical and dianion. A similar result was obtained for the consecutive one electron reduction of (P)[Rh(CO)₂]₂. ESR evidence also supports the site of electron transfer to be the porphyrin π-ring system. Frozen solutions of (TPP)[Ir(CO)₃]₂ in PhCN containing 0.2 M TBAP were electrolyzed at –1.20 V and gave an ESR

spectrum very similar to the one obtained after the one-electron reduction of (P)[Rh(CO)₂]₂ under similar solution conditions.[17] An assymetric signal for (TPP)[Ir(CO)₃]₂⁻ was found with $g_\perp$ = 2.00 and $g_\parallel$ = 1.88. The peak to peak width for $g_\perp$ is 27 G, and the total signal width of $g_\parallel$ is 347 G. Similar to the reduced rhodium porphyrin species, the assymetric signal of (TPP)[Ir(CO)₃]₂⁻ is due to the overall lower symmetry of the complex which has one metal carbonyl unit above and the other below the porphyrin plane.

Electrooxidation of (TPP)[Ir(CO)₃]₂. The oxidation waves observed for solutions of (TPP)[Ir(CO)₃]₂ both in CH₂Cl₂ (processes 3 and 4 in Figure 1a) and in PhCN (processes 3, 4, and 5 in Figure 1b) are irreversible in that there are no rereduction peaks associated with these oxidations. The current for process 4 is larger than that for process 3, and, in PhCN, process 4 appears to consist of two overlapping reactions. These overlapping reactions are clearly shown by the differential pulse voltammogram in Figure 1c.

Oxidation process 3 has a much smaller peak current by differential pulse voltammetry compared to the peak current for oxidation process 4 or the peak current for the reduction processes 1 and 2. However, bulk electrolysis and thin-layer coulometry give 1.0 ± 0.1 electron abstracted in process 3 and 1.6 ± 0.1 electrons abstracted in the overall process 4.

The first oxidation of (TPP)[Ir(CO)₃]₂ involves a diffusion-controlled, one-electron transfer followed by a chemical reaction, i.e. an electrochemical EC mechanism. The reversible nature of the electron transfer is demonstrated by the measured $|E_p - E_{p/2}|$ = 60 ± 5 mV and the constant value of $i_p/v^{1/2}$ in both CH₂Cl₂ and PhCN. The oxidation of (TPP)[Ir(CO)₃]₂ in CH₂Cl₂ remains irreversible at all temperatures between 23 and –78 °C, thus indicating that the coupled chemical reaction is much faster than the preceding electron-transfer process that could not be isolated at low temperature.

The homogeneous chemical reaction following the first oxidation of (TPP)[Ir(CO)₃]₂ in benzonitrile generates monomeric [(TPP)Ir]⁺ClO₄⁻. This assignment is based on results from electrochemical and spectroelectrochemical data taken under various conditions and described in the following sections. Although only slight differences in the UV–vis spectra are observed when [(TPP)Ir]⁺ClO₄⁻ is generated in different solvent systems, this species is probably solvated and the formation of [(TPP)Ir(S)]⁺ and/or [(TPP)Ir(S)₂]⁺ (where S is a solvent molecule) is possible. This solvation is consistent with the tendency for cationic metalloporphyrin species to coordinate one or more solvent molecules.[22] However, in order to avoid confusion as to the exact nature of the monooxidized species in solution, we have designated it as [(TPP)Ir]⁺·ClO₄⁻. [(TPP)Ir]⁺ClO₄⁻ is reactive and the resulting formation of [(TPP)Ir(CO)]⁺, (TPP)IrCl, or (TPP)Ir(CO)Cl from this species is possible.

UV–visible spectral changes during oxidation of (TPP)[Ir(CO)₃]₂ at +1.2 V in PhCN containing 0.2 M TBAP are shown in Figure 3a. Isobestic points are located at 370, 424, 505, and 543 nm, indicating only two absorbing species in equilibrium. The initial absorbances of the binuclear complex at 360, 457, 564, 614, and 662 nm decrease in intensity during the first oxidation, and new absorption peaks appear at 416 and 527 nm. In CH₂Cl₂, this species has bands at 413 and 524 nm and suggest solvation by either CH₂Cl₂ or PhCN. These spectra are
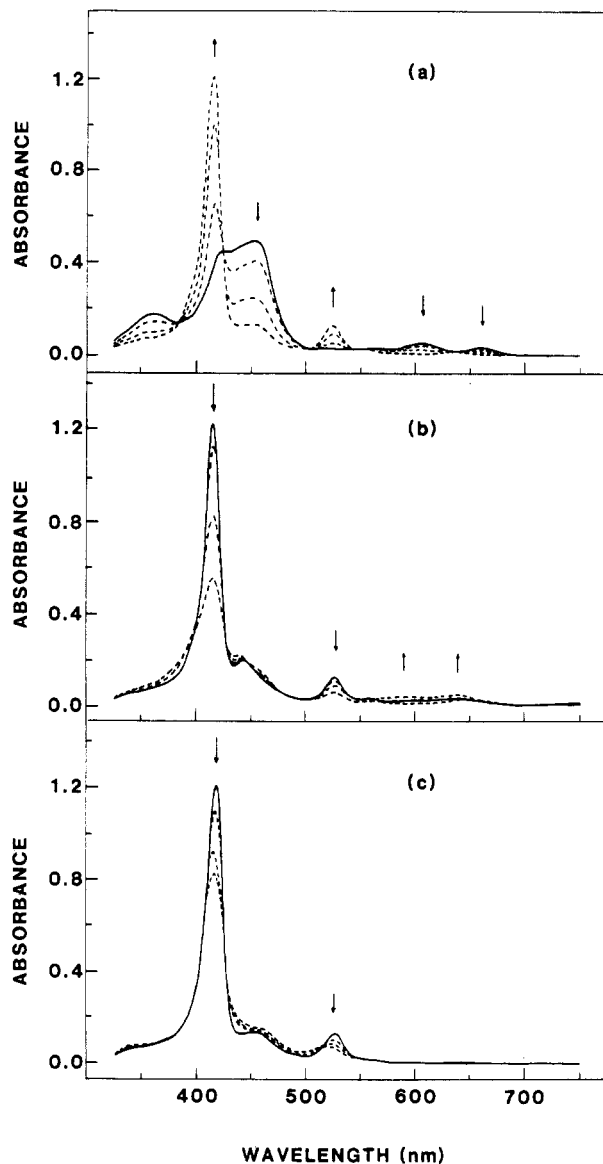
(22) Kadish, K. M. *Prog. Inorg. Chem.* **1986**, *34*, 435–605.

Figure 3. UV–visible spectral changes during controlled potential oxidation of 1.6×10^{-4} M $(TPP)[Ir(CO)_3]_2$ in PhCN, 0.2 M TBAP, at (a) +1.20 V, (b) upon stepping the potential from +1.20 to +1.50 V, and (c) upon stepping the potential from +1.20 to –0.90 V.

POTENTIAL (V vs SCE)

Figure 4. (a) Conventional cyclic voltammogram of 8.2×10^{-4} M $(TPP)[Ir(CO)_3]_2$ in PhCN, 0.2 M TBAP (scan rate = 0.1 V/s) and (b) thin-layer cyclic voltammogram of 4.8×10^{-4} M $(TPP)[Ir(CO)_3]_2$ under the same solution conditions (scan rate = 0.01 V/s). Data are shown for the first (—) and the second (- - -) scan.

characteristic of a monometallic Ir(III) porphyrin,[14,21] and no ESR signal is found following the initial oxidation.

The absorption bands of the oxidation product at 416 and 527 nm are assigned to $[(TPP)Ir]^+ClO_4^-$. These bands decrease in intensity and are accompanied by the appearance of broad absorbances at 582 and 635 nm during the second controlled potential oxidation at +1.50 V in PhCN, 0.2 M TBAP. This is shown in Figure 3b. The same types of spectral changes have been reported during oxidation of $(TPP)Ir(CO)Cl^{21}$ and are typical for formation of a porphyrin π-cation radical. Similar spectral changes occur during controlled potential oxidation of $(TPP)[Ir(CO)_3]_2$ in PhCN and CH_2Cl_2, and spectral data for the oxidized complexes in both solvents are listed in Table I.

The initial $(TPP)[Ir(CO)_3]_2$ complex has IR peaks due to carbonyl stretching frequencies at 2054 and 1979 cm^{-1}. Both bands decrease in intensity during controlled potential oxidation at +1.16 V (vs Ag/AgCl), and this suggests that CO is lost as the complex is oxidized. The porphyrin product isolated after bulk electrolysis has no IR stretches that can be assigned to CO, and this also suggests a cleavage of the Ir–CO bonds during oxidation. Furthermore, the UV–visible spectroelectrochemical data
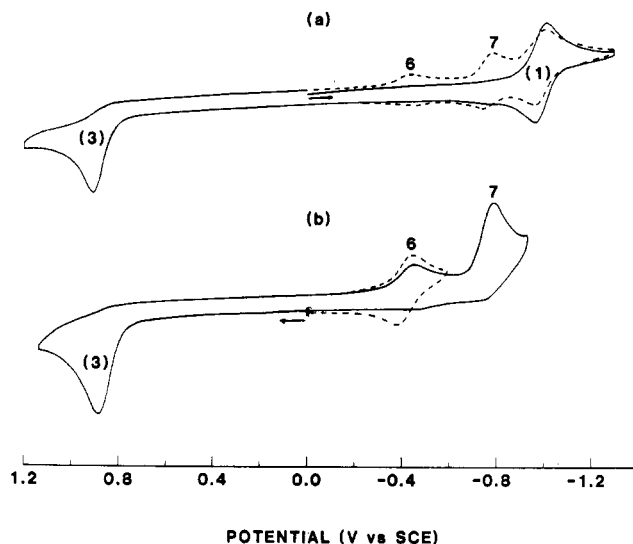
suggests that $[(TPP)Ir]^+ClO_4^-$ is the only porphyrin product formed in the electrooxidation.

Two reversible reduction waves at $E_{1/2}$ = –0.43 and –0.77 V are observed after the first electrooxidation of $(TPP)[Ir(CO)_3]_2$ in PhCN. These reductions are shown by a dashed line and labeled as processes 6 and 7 in Figure 4a. Both reductions are reversible by conventional cyclic voltammetry but only process 6 is reversible on the thin-layer cyclic voltammetric time scale (Figure 4b). No UV–visible spectral changes occur when the electrode potential is stepped from +1.2 (a potential sufficient for the first oxidation) to –0.60 V (a potential between processes 6 and 7). However, the bands of $[(TPP)Ir]^+ClO_4^-$ at 416 and 527 nm decrease in intensity upon applying a controlled potential of –0.90 V. (This potential is negative of peak 7.) These spectral changes are shown in Figure 3c. The final UV–visible spectrum after total reduction at –0.90 V is similar, but not identical, to that of $[(TPP)Ir]^-$, a species which has been characterized in a previous study.[21]

In summary, the spectroelectrochemical data suggest that processes 6 and 7 are due to reduction of two different species in solution, only one of which is a metalloporphyrin. The metalloporphyrin is assigned as $[(TPP)Ir]^+ClO_4^-$ and is reduced in process 7. The species reduced in process 6 is assigned as a non-porphyrin iridium complex, since a similar reduction is observed at $E_{1/2}$ = –0.44 V after oxidation of $[Ir(CO)_3Cl]_2$ at 0.60 V in CH_2Cl_2 containing 10% methanol. This assignment is consistent with the fact that there are no changes in the porphyrin-dominated UV–visible spectra as the electrode potential in the thin-layer cell is scanned through process 6.

Process 7 is located at $E_{1/2}$ = –0.77 V in PhCN (see Figure 4a). This reduction peak decreases in intensity, and a new peak at $E_{1/2}$ = –1.14 V appears in the cyclic voltammogram when TBACl is titrated into solutions of $(TPP)[Ir(CO)_3]_2$. The current voltage curve in the presence of 2 equiv of TBACl is identical with that for $(TPP)Ir(CO)Cl$ which is reduced at $E_{1/2}$ = –1.15 V in CH_2Cl_2,[21] thus strongly suggesting that this species is formed under these experimental conditions. Also, the reduction wave at $E_{1/2}$ = –0.77 V shifts to $E_{1/2}$ = –0.94 V upon bubbling CO through a PhCN solution containing 0.2 M TBAP. This suggests that $[(TPP)Ir(CO)]^+ClO_4^-$ is formed from $[(TPP)Ir]^+ClO_4^-$ under a CO atmosphere.

$(TPP)[Ir(CO)_3]_2 \underset{(1)}{\overset{e}{\rightleftharpoons}} (TPP)[Ir(CO)_3]_2^- \underset{(2)}{\overset{e}{\rightleftharpoons}} (TPP)[Ir(CO)_3]_2^{2-}$

$(TPP)[Ir(CO)_3]_2 \underset{(3)}{\overset{-e,\ Chem\ Rxn}{\longrightarrow}} [(TPP)Ir]^+ \underset{(4)}{\overset{-e}{\longrightarrow}} [(TPP)Ir]^{2+}$

$[(TPP)Ir]^+ClO_4^- \qquad [(TPP)Ir(CO)]^+ClO_4^- \qquad (TPP)Ir(CO)Cl$
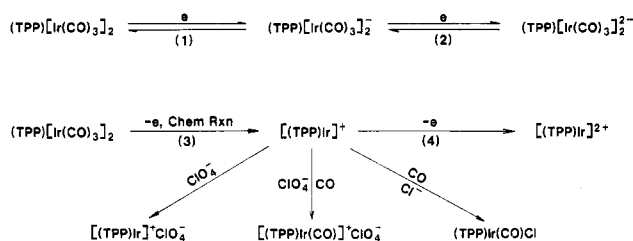
Figure 5. Overall mechanism for the oxidation and reduction of $(TPP)[Ir(CO)_3]_2$. Numbers 1–4 correspond to processes in the cyclic voltammograms illustrated in Figure 1. The possible solvation of $[(TPP)Ir]^+$ is omitted for clarity.

Overall Reaction Scheme for $(TPP)[Ir(CO)_3]_2$. The overall reaction scheme of $(TPP)[Ir(CO)_3]_2$ in PhCN and CH_2Cl_2 is summarized in Figure 5. $(TPP)[Ir(CO)_3]_2$ can undergo two consecutive reductions at the porphyrin π-ring system to form an anion radical and a dianion. This electron-transfer mechanism is supported by the electrochemical and spectroelectrochemical data as well as by the ESR spectra recorded after bulk solution electrolysis.

The first oxidation of $(TPP)[Ir(CO)_3]_2$ is followed by a chemical reaction to generate $[(TPP)Ir]^+ClO_4^-$ in PhCN, 0.2 M TBAP. Similar types of reactions have been reported for $(TPP)[Rh(CO)_2]_2^{17}$ which, upon oxidation, generates a transient Rh^{II}–Rh^I complex followed by an intramolecular electron transfer to form $[(TPP)Rh]^+ClO_4^-$ and elemental rhodium metal. The formation of $[(TPP)Ir]^+ClO_4^-$ following the one-electron oxidation of $(TPP)[Ir(CO)_3]_2$ would also require the transfer of a second electron, presumably from the second iridium atom. However, iridium metal was not clearly isolated in the present study, and positive identification of the second electron source has not been made.

In summary, the electrochemical properties of (TPP)-$[Ir(CO)_3]_2$ are almost identical with the properties of $(TPP)[Rh(CO)_2]_2$. The first reduction of both binuclear complexes reversibly occurs at the porphyrin π-ring system. The values of $E_{1/2}$ are similar and occur at –0.99 V for $(TPP)[Ir(CO)_3]_2$ and –1.04 V for $(TPP)[Rh(CO)_2]_2$ in benzonitrile. The first oxidation of both binuclear complexes is irreversible and occurs at $E_p = 0.92$ V for $(TPP)[Ir(CO)_3]_2$ and $E_p = 0.84$ V for $(TPP)[Rh(CO)_2]_2$ in benzonitrile at a scan rate of 0.1 V/s.[17] The electrooxidation of each compound involves the overall conversion of a metal(I) to a metal(III) ion and the ultimate formation of $[(P)M]^+$. However, unlike $(TPP)[Rh(CO)_2]_2$ which can be reversibly oxidized at low temperature or fast scan rates, the chemical reaction or reactions following electron abstraction from $(TPP)[Ir(CO)_3]_2$ are extremely rapid and in no case could reversible electrooxidations be obtained.

Kinetic and Thermodynamic Acidity of Hydrido Transition-Metal Complexes. 5. Sensitivity of Thermodynamic Acidity to Ligand Variation and Hydride Bonding Mode

Sigríður S. Kristjánsdóttir, Anne E. Moody, Rolf T. Weberg, and Jack R. Norton*

Department of Chemistry, Colorado State University, Fort Collins, Colorado 80523

Received December 21, 1987

The pK_a values of $CpRe(CO)_2H_2$, $(\eta^3-C_6H_9)Mn(CO)_3$, $(\eta^6-C_6H_6)Mn(CO)_2H$, $HMn(CO)_4(PPh_3)$, $HMn(CO)_4(PEtPh_2)$, $(\mu-H)_2Fe_3(CO)_9(\mu_3-P-t-Bu)$, $(\mu-H)_2Fe_3(CO)_9(\mu_3-P-p-C_6H_5OCH_3)$, $(\mu-H)Fe_3(CO)_9(\mu_3-SC_6H_{11})$, $H_4Ru_4(CO)_{11}(P(OCH_3)_3)$, and $H_4Ru_4(CO)_{10}(P(OCH_3)_3)_2$ have been determined in acetonitrile by IR measurement of the position of deprotonation equilibria with various nitrogen bases and sodium phenolate. The acidity of transition-metal hydrides appears more sensitive to the nature of the ancillary ligands than to the identity of the metal center.

We have reported the thermodynamic acidity of common mononuclear transition-metal hydrides in acetonitrile.[1] These results have enabled us to quantify periodic trends and some substituent effects. Our work has been carried out in acetonitrile for several reasons: it dissolves most metal hydrides without decomposition and solvates cations effectively; it minimizes ion pairing; and, as it is both a weak acid and a weak base, a large range of pK_a values can be measured in it.

We have now extended our initial studies to compounds containing other types of hydride ligands, e.g., to agostic and edge-bridging hydrides. We have also investigated the sensitivity of hydride pK_a values to small changes in the nature of ancillary phosphine ligands.

We have examined the edge-bridging hydrides in the $H_4Ru_4(CO)_{12-x}(P(OCH_3)_3)_x$ of tetranuclear ruthenium hydride clusters because Pearson and Ford[2] had previously studied their thermodynamic and kinetic acidities in

(1) (a) Jordan, R. F.; Norton, J. R. *J. Am. Chem. Soc.* 1982, *104*, 1255. (b) Jordan, R. F.; Norton, J. R. *ACS Symp. Ser.* 1982, *No. 198*, 403. (c) Moore, E. J.; Sullivan, J. M.; Norton, J. R. *J. Am. Chem. Soc.* 1986, *108*, 2257. (d) Edidin, R. T.; Sullivan, J. M.; Norton, J. R. *J. Am. Chem. Soc.* 1987, *109*, 3945. These are the first four papers in a series of which the present is part 5.

(2) (a) Walker, H. W.; Kresge, C. T.; Pearson, R. G.; Ford, P. C. *J. Am. Chem. Soc.* 1979, *101*, 7428. (b) Walker, H. W.; Pearson, R. G.; Ford, P. C. *J. Am. Chem. Soc.*, 1983, *105*, 1179.